



Genetic architecture of disease resistance and tolerance in Douglas-fir trees

Pooja Singh^{1,2,3} , J. Bradley St Clair⁴, Brandon M. Lind⁵ , Richard Cronn⁴ , Nicholas P. Wilhelm⁶, Nicolas Feau⁵ , Mengmeng Lu¹ , Dragana Obreht Vidakovic⁵, Richard C. Hamelin⁵ , David C. Shaw⁷, Sally N. Aitken⁵  and Sam Yeaman¹ 

¹Department of Biological Sciences, University of Calgary, Calgary, AB, T2N 1N4, Canada; ²Aquatic Ecology & Evolution Division, Institute of Ecology and Evolution, University of Bern, Bern, CH-3012, Switzerland; ³Department of Fish Ecology & Evolution, Swiss Federal Institute of Aquatic Science and Technology (EAWAG), Kastanienbaum, CH-6047, Switzerland; ⁴USDA Forest Service, Pacific Northwest Research Station, 3200 SW Jefferson Way, Corvallis, OR 97331, USA; ⁵Department of Forest and Conservation Sciences, University of British Columbia, Vancouver, V6T1Z4, BC, Canada; ⁶Forest Health Protection, USDA Forest Service, Arizona Zone, Flagstaff, AZ 86001, USA; ⁷Department of Forest Engineering, Resources and Management, Oregon State University, Corvallis, OR 97331, USA

Summary

Authors for correspondence:

Pooja Singh

Email: pooja.singh09@gmail.com

Sam Yeaman

Email: samuel.yeaman@ucalgary.ca

Received: 4 January 2024

Accepted: 18 March 2024

New Phytologist (2024) **243**: 705–719

doi: 10.1111/nph.19797

Key words: climate change, disease resistance, Douglas-fir, fungal pathogens, GWAS, local adaptation, temperate trees.

- Understanding the genetic basis of how plants defend against pathogens is important to monitor and maintain resilient tree populations. Swiss needle cast (SNC) and Rhabdocline needle cast (RNC) epidemics are responsible for major damage of forest ecosystems in North America.
- Here we investigate the genetic architecture of tolerance and resistance to needle cast diseases in Douglas-fir (*Pseudotsuga menziesii*) caused by two fungal pathogens: SNC caused by *Nothophaeocryptopus gaeumannii*, and RNC caused by *Rhabdocline pseudotsugae*.
- We performed case-control genome-wide association analyses and found disease resistance and tolerance in Douglas-fir to be polygenic and under strong selection. We show that stomatal regulation as well as ethylene and jasmonic acid pathways are important for resisting SNC infection, and secondary metabolite pathways play a role in tolerating SNC once the plant is infected. We identify a major transcriptional regulator of plant defense, ERF1, as the top candidate for RNC resistance.
- Our findings shed light on the highly polygenic architectures underlying fungal disease resistance and tolerance and have important implications for forestry and conservation as the climate changes.

Introduction

Douglas-fir (*Pseudotsuga menziesii*) is a foundational species in western North America, found in abundance both in coastal rainforests (var. *menziesii*) and in drier, warm continental climates (var. *glauca*). It is one of the most valuable timber trees and a keystone species in several forest ecosystems. Anthropogenic factors, such as climate change, threaten the health and productivity of Douglas-fir in its native and non-native range. Pathogens also pose an unprecedented threat to our natural and commercially valuable forests (Smith *et al.*, 2006). Several plant pathogens cause diseases that are known to be exacerbated by climate change, with an increase in epidemics predicted in the future (Bergot *et al.*, 2004; Evans *et al.*, 2008; Juroszek *et al.*, 2020). Identifying genetic variation underlying disease resistance is crucial to estimate the adaptive potential of plants and select for resistant genotypes. Swiss needle cast (SNC), caused by *Nothophaeocryptopus gaeumannii*, and Rhabdocline needle cast (RNC), caused by *Rhabdocline pseudotsugae*, are two such pathogens

causing diseases exclusive to the widespread ecologically and economically important conifer species Douglas-fir (Boyce, 1940; Chastagner, 2001).

Swiss needle cast (SNC) is thought to be native to Douglas-fir trees in North America (Boyce, 1940) but was first described in Switzerland in 1925 and has since spread across the globe, to wherever Douglas-fir is grown (Stone, 2018). The impact of SNC is most severe in the coastal fog zone of British Columbia, Washington, and Oregon (Fig. 1a) and has worsened over the last 40 yr (Hansen *et al.*, 2000; Black *et al.*, 2010; Shaw *et al.*, 2021). *Nothophaeocryptopus gaeumannii* thrives in humid conditions that are found where the coastal variety *P. menziesii* var. *menziesii* grows. During *N. gaeumannii* infection, pseudothecia occlude Douglas-fir stomata (Fig. 1b), reducing CO₂ uptake (Capitani, 1999; Manter *et al.*, 2003). Once 25% of the stomata are occluded, net CO₂ uptake approaches zero, needle retention decreases and chlorosis increases (Manter *et al.*, 2000, 2003; Ritóková *et al.*, 2016). This inevitably results in reduction in tree growth, but tree mortality as a result is rare (Shaw *et al.*, 2011).

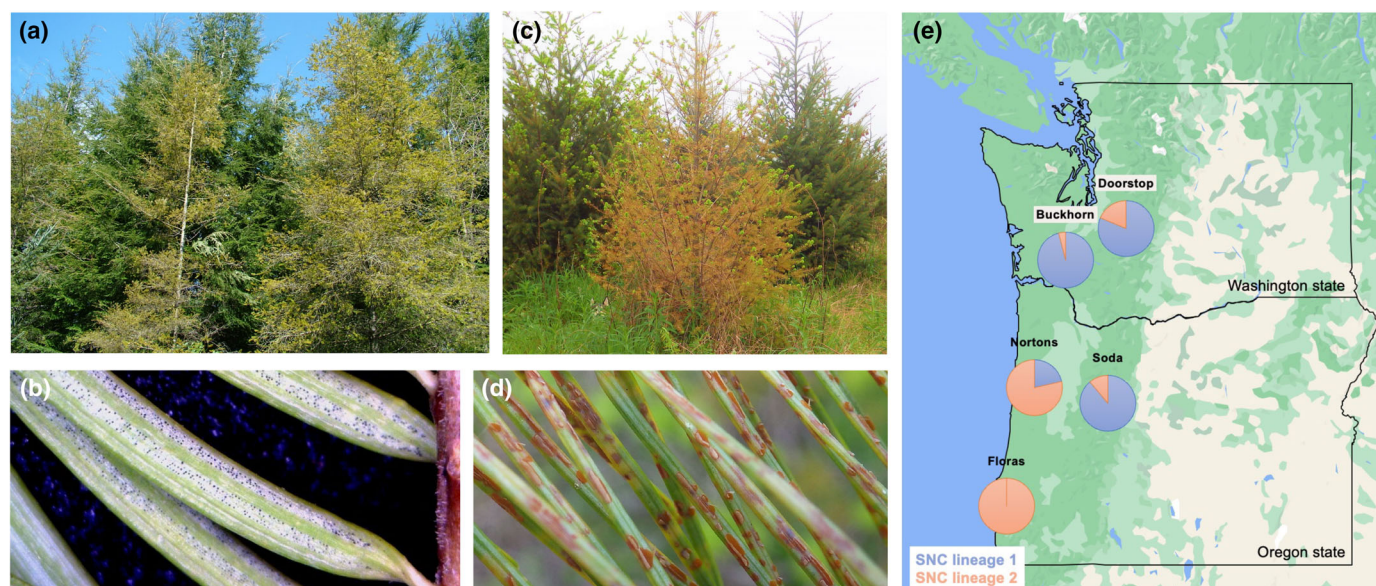


Fig. 1 Damage in coastal Douglas-fir (*Pseudotsuga menziesii* var. *menziesii*) trees from (a) Swiss needle cast (SNC) disease caused by *Nothophaeocryptopus gaeumannii* that results in poor foliage retention. (b) *Nothophaeocryptopus gaeumannii* infected Douglas-fir needles. Fruiting fungal bodies (pseudothecia) appear black and occupy stomata. (c) Heavily infected Douglas-fir tree by *Rhabdocline* needle cast (RNC) disease caused by *Rhabdocline pseudotsugae*. (d) *Rhabdocline pseudotsugae* causes reddish-brown blotches on infected needles, followed by defoliation, growth loss, and eventual tree mortality. (e) Distribution of SNC lineages identified at planting sites in Pacific Northwestern USA investigated in this study.

Local climate likely plays a role in the pathogenicity of *N. gaeumannii* because the most severe symptoms are found in the low-elevation coastal fog zone and infections have increased in severity in these zones since 1980 (Black *et al.*, 2010). Disease prediction models have found that warmer winters and higher spring and summer precipitation in previous years strongly correlates with SNC abundance and severity in the following years (Stone *et al.*, 2008; Wilhelmi *et al.*, 2017). As much as 50% growth loss has been reported in coastal Douglas-fir since 1990 from SNC epidemics (Maguire *et al.*, 2002; Shaw *et al.*, 2021). The resulting reduction in CO₂ fixation is a global concern because Douglas-firs represent a major terrestrial carbon sink. With climate change resulting in warmer temperatures, *N. gaeumannii* severity is projected to expand and become a major environmental challenge beyond the coastal fog belt (Lee *et al.*, 2017). Recently, two major sympatric genetic lineages of *N. gaeumannii* were identified in the coastal Pacific Northwest. A distribution modelling approach suggested that the environmental tolerance range of lineage 1 exceeds that of lineage 2 and that lineage 1 should expand inland while distribution of lineage 2 should remain limited to its current range (Herpin-Saunier *et al.*, 2022).

Douglas-fir is host to another foliar fungal pathogen, *R. pseudotsugae*, which causes RNC in the coastal Pacific Northwest United States and Canada (Chastagner, 2001; Fig. 1c,d) and has spread to Europe. The infection by *R. pseudotsugae* is thought to be associated with local environments, particularly moisture (Wilhelmi *et al.*, 2017, 2021). *Rhabdocline* spp. require similar environmental conditions as *N. gaeumannii* with high humidity, rain, and mild temperatures most conducive to infection (Parker, 1970; Chastagner *et al.*, 1990). Unlike

N. gaeumannii, *Rhabdocline* spp. infection takes place directly through the cuticle of the needle (Brandt, 1960) and it kill host cells as it progresses. This produces mottled chlorosis and necrotic spots that coalesce giving the foliage a characteristic chlorotic yellow to light brown color. Needles are generally cast in the early summer, shortly before or after fruiting bodies emerge (Brandt, 1960; Chastagner *et al.*, 1990; Wilhelmi *et al.*, 2021). Decreases in growth due to the loss of foliage related to *Rhabdocline* infection are estimated to be as high as 50% for trees with moderate to severe infection (Kurkela, 1981).

A tractable approach to improve tree health and resilience to pathogens is to understand and deploy the innate tolerance and resistance mechanisms of trees. Plant resistance mechanisms reduce the probability of pathogen infection and tolerance mechanisms reduce loss of fitness even when infected (Restif & Koella, 2004). Hereafter we refer to 'resistance' as the tree defense responses that reduce pathogen abundance and 'tolerance' as the tree's ability to continue to grow and retain its leaves, even in the presence of the pathogen, *sensu* Wilhelmi *et al.* (2017). In coastal Douglas-fir populations where SNC infections can be severe, trees have evolved resistance as well as tolerance to SNC (Shaw *et al.*, 2011; Lee *et al.*, 2017). Wilhelmi *et al.* (2017) found evidence for genetic variation across populations in the Pacific Northwest for SNC tolerance (but not resistance) and RNC resistance. This local adaptation for SNC tolerance and RNC resistance is consistent with how plant pathosystems evolve (Croll & McDonald, 2017). Plant populations under stronger pathogen pressure evolve higher tolerance/resistance to the pathogen. Therefore, local adaptation plays a key role in the evolutionary trajectory of plant–pathogen interactions. The difference in tolerance/resistance between SNC and RNC is attributed to their

different infection modes: *R. pseudotsugae* is a necrotroph that kills host cells to feed while *N. gaeumannii* is a biotroph that is endophytic and its nutrition depends on living host cells (Brandt, 1960; Capitano, 1999). Like SNC, RNC resistance is also known to have a genetic basis (Wilhelmi *et al.*, 2017, 2021; Stone, 2018). Even though the epidemiology and pathogenicity of these two needle cast diseases are well studied, the molecular genetic basis of resistance and tolerance to infection is poorly understood.

Genome-wide association studies (GWAS) have played a crucial role in identifying the genetic regions associated with disease resistance in plants (Zhu *et al.*, 2008). Here, we employ a GWAS approach to understand the genomic basis of tolerance and resistance to needle cast fungal diseases in Douglas-fir trees from Northwestern USA. Our statistical analysis has been adapted for Douglas-fir exome pooled-sequencing data from multiple populations with 4–20 individuals per population. A case-control design compares allele frequencies between a group of disease resistant (or tolerant) individuals (cases) and a group of disease intolerant individuals (controls). Our aim was to shed light on the genetic architecture of disease tolerance and resistance in Douglas-fir and identify candidate genes that play an adaptive role in fighting off SNC and RNC. The resistant and tolerant SNPs from our study have been included in a SNP array for use in genomic selection in forestry management and conservation of Douglas-fir (B. M. Lind *et al.*, in preparation).

Materials and Methods

Sampling, study design, and disease phenotyping

A Seed Source Movement Trial (SSMT) was used to evaluate resistance and tolerance to natural infections of SNC and RNC by local fungal strains in 60 Douglas-fir populations (seed sources) from 12 geographic regions in Oregon, Washington, and California (see Wilhelmi *et al.*, 2017 for details, Fig. 1e, Supporting Information Fig. S1; Table S1 have sampling and location information). Foresters use SSMTs to test seed sources to make decisions about planting locations where the seed source environment and the future climate will be similar. SSMTs are also known as ‘assisted migration’ with the idea that we are assisting plants move to better suited environments faster than they would naturally. Each of the 12 regions included samples from five populations, with samples from each population consisting of open-pollinated seed from two parent trees naturally regenerated within a stand (Table S1). Parents were located 100 m apart to avoid sampling close relatives. The seed source regions and test sites were used to capture the climatic gradients experienced by *P. menziesii* var. *menziesii*. 7040 1 yr old trees were planted in the nine common gardens (test sites) and surveyed after 7 yr (8 yr old), with different subsets of these test sites included in the SNC/RNC sequencing pools, as described below. Notes S1 contains the protocol of tree health phenotyping by foresters for this study. Trees were not artificially infected and were exposed to naturally occurring levels of SNC/RNC inoculum/infection in

nature. The timing and level of inoculum is consistent within a test site but differences in climate, infection timing, and level of inoculum will vary from site to site.

A two-step process was used to classify individuals into the ‘resistant’ (R), ‘tolerant’ (T), and ‘intolerant’ (I) SNC groups within each combination of planting site and seed source region using the tree health phenotypes assigned by foresters. First, individuals were classified into the resistant group based on the severity of SNC infection, assessed as the proportion of stomata that were occluded by pseudothecia, using measurements from two secondary lateral branches on the fourth whorl from the top of the tree, one from the North and one from the South side of the tree. Individuals with no or very few pseudothecia present on the underside of the needle were classified as resistant (a score of 0 or 1 out of 3), with no more than two individuals per family included in a site \times region group. In many of the site \times region groups, there was an insufficient number of resistant individuals to form a pool for sequencing, so only 13 site \times region resistant pools were sequenced. Within each site \times region group, from individuals falling into the top 75% by stomatal occlusion, trees were further classified into ‘tolerant’ and ‘intolerant’ groups based on an overall health index combining the following phenotype criteria: (A) Crown density rated on a scale ranging from 1 to 4, with a 1 corresponding to an unhealthy, sparse crown lacking in needle retention and a 4 corresponding to a full healthy crown (note: this estimate is a function of all the infections (every spring) that have occurred since planting and individual tree tolerance/resistance to infection); (B) Crown color rated on a scale from 1 to 3, with 1 corresponding to highly chlorotic crown color and 3 corresponding to a healthy green crown color; and (C) Needle retention rated on a secondary lateral branch located on the fourth whorl and on the south side of the tree, and was estimated as the proportion of needles retained in each year of growth (e.g. 1.5 refers to a tree holding 100% of its current year needles, 50% of its second-year needles and no third-year needles). As crown density was considered the most representative measure, the index of overall health was calculated as: $2 \times \text{Crown density} + \text{Crown color} + \text{Needle retention}$. Pools of tolerant and intolerant individuals were constructed within each site \times region combination by picking the highest- and lowest-ranked individuals from each family using this health index (note that the cutoffs for these rankings can, therefore, vary among site \times region combinations; Fig. S2). For the RNC analysis, infection severity was assessed as a single index from 0 (most severe) to 3 (least severe). Pooling for RNC was conducted as above, but there were fewer populations infected so fewer pools could be included. The final set of site \times region combinations included in our study come from 5 out of 9 of the planting sites and 11 out of the 12 seed source regions (see Dryad repository for detailed list); three California planting sites were excluded due to limited prevalence of SNC, one planting site was excluded for logistical reasons associated with sampling DNA, and one region was excluded due to extreme rhabdocone infection. The R script used to calculate severity indices and assign resistant/tolerant/intolerant phenotypes is included in the Dryad repository (categorising_infection_severity.R). Fig. S2 illustrates health

index of SNC tolerant and intolerant individuals selected for each site.

Probe design and sequencing

We used a pool-sequencing approach that targeted exon regions. For probe design details see Lind *et al.* (2022). Briefly, the sequence capture probes were designed using 37 787 genes identified in Douglas-fir RNA-Seq data from (1) daily and cyclic-induced experiments (Cronn *et al.*, 2017) and (2) needles samples infected by the fungal pathogen causing SNC *N. gaeumannii* (Lind *et al.*, 2022). Exon sequences with a length of at least 100 bp were submitted to Roche NimbleGen for Custom SeqCap EZ probe design.

For pool-seq, DNA was extracted from newly expanded Douglas-fir needles to ensure low hyphal load. DNA samples were normalized at $c. 10 \text{ ng } \mu\text{l}^{-1}$ and 4–20 individuals were pooled per site (see Table S2 for DNA concentrations and ploidy of pools) by combining equimolar amounts of individual DNA samples prior to library preparation. Barcoded (Roche Diagnostics Corp., Indianapolis, IN, USA) libraries were made using 100–150 ng of DNA from each pooled DNA sample with an $c. 450\text{-bp}$ mean insert size. SeqCap library preparation was performed using custom NimbleGen SeqCap probes according to the NimbleGen SeqCap EZ HyperCap Workflow User's Guide v.2 (Roche Sequencing Solutions Inc., Pleasanton, CA, USA). Following capture, each library was sequenced in a 150 bp paired-end format on an Illumina NovaSeq 6000 instrument at the Genome Quebec Innovation Centre (McGill University, Montreal, QC, Canada).

Mapping and SNP calling

As in Lind *et al.* (2022), we used the VarScan pipeline (Lind, 2022) to process our genomic data. Raw sequence reads were trimmed with FASTP (v.0.19.5; Chen *et al.*, 2018) by trimming reads that did not pass quality filters of $< 20 \text{ N's}$, a minimum mean PHRED quality score of 30 for sliding windows of 5 bp, and a final length of 75 bp with no more than 20 bp called as N ($-n 20 -M 30 -W 5 -l 75 -g -3$). Trimmed reads were mapped with BWA-MEM (v.0.7.17; Li & Durbin, 2009) to the congeneric Douglas-fir *P. menziesii* var. *menziesii* reference (v.1.0) (Wegrzyn *et al.*, 2014). This reference was extended by including nonredundant contigs from an in-house Douglas-fir SNC infected needle transcriptome assembly. See Extended annotation section below for details on the extended reference. The mapped read .sam files were converted to binary with SAMTOOLS v.1.9 (view, sort, index; Li *et al.*, 2009) and subsequently filtered for proper pairs and a mapping quality score of 20 or greater (view $-q 20 -f 0x0002 -F 0x0004$). Using PICARD tools v.2.18.9 (<http://picard.sourceforge.net>), read groups were added and duplicates subsequently removed from filtered bam files. Indel realignment was performed with GATK 3.8 (McKenna *et al.*, 2010). SNP calling was done using VarScan (v.2.4.3; Koboldt *et al.*, 2012) by passing a SAMTOOLS mpileup object directly to VarScan::mpileup2cns with a minimum coverage set to 8, $P\text{-value} < 0.05$ from a Fisher exact test on observed vs

expected read counts for nonhomozygous calls (given sequencing error), minimum variant frequency of 0.00, ignoring variants with $< 90\%$ support on one strand, a minimum average genotype quality of 20, and a minimum allele frequency of 0.80 to call a site homozygous ($--\text{min-coverage } 8 --P\text{-value } 0.05 --\text{min-var-freq } 0.00 --\text{strand-filter } 1 --\text{min-avg-qual } 20 --\text{min-freq-for-hom } 0.80$). Global allele frequency was calculated by multiplying each pool's ploidy ($2n$) by the pool's ALT allele frequency, summing these products, and dividing by the total ploidy across populations. The output was filtered with a custom PYTHON (v.3.7, www.python.org) script to remove indels, keeping only biallelic loci, genotype quality score > 20 , and filter for global minor allele frequency ≥ 0.05 . SNP contingency tables were generated by calculating REF/ALT allele counts by multiplying the total ploidy of the pool ($2 \times$ number of individuals) by the ALT allele frequency or $1 - \text{ALT allele frequency}$. SNPs flagged as being paralogs by were discarded. Paralogous regions were identified using Douglas-fir haploid megagametophyte data from Douglas-fir data, where apparent heterozygous regions represent collapsed paralogs, see Lind *et al.* (2022) for details. Code for the SNP calling pipeline can be found here: https://GitHub.com/CoAdapTree/varscan_pipeline.

Cochran–Mantel–Haenszel (CMH) test

A case–control method was implemented to identify loci associated with SNC and RNC tolerance/resistance. Using output from the VarScan pipeline (Lind, 2022) we performed GWAS using a modified Cochran–Mantel–Haenszel (CMH) test implemented in PYTHON (Lind, 2023) across stratified contingency tables. Here, each stratum pertains to a single population (i.e. site \times region combination), where each population has a 'case' and a 'control' pool. In every comparison, 'case' was always the most affected group and 'control' was always the least affected group. Each contingency table is 2×2 – case and control \times REF and ALT allele counts. ALT and REF allele counts are calculated by multiplying the ploidy of the pool ($2n$) by either the ALTfreq or $(1 - \text{ALTfreq})$, respectively. This step converts read depth into pseudo-counts, which represent our real replication level. Pseudo-counts are necessary because sequencing coverage per pool exceeds the number of individuals in each pool, resulting in resampling of same allele from a single individual several times. Our tested case–control comparisons for SNC were as follows: (1) Intolerant vs Tolerant, (2) Tolerant vs Resistant, and (3) Intolerant vs Resistant comparisons. SNC Tolerant vs Resistance comparison was included for completeness on the off chance that there were any important GWAS signals that differentiated trees that had lowest amounts of SNC damage from those that were intermediate. For RNC, susceptible vs resistant groups were contrasted to identify SNPs associated with resistance. Code for the CMH pipeline is available here: https://github.com/CoAdapTree/cmh_test. False discovery rate (FDR) correction was applied with a threshold of < 0.05 for significance. Finally, we tested for enrichment in outlier status between groups of SNPs identified among the three SNC case–control comparisons using the hypergeometric test in R v.4.0.5.

Extended annotation and Gene Ontology enrichment

The existing Douglas-fir genome annotation (v.1.0) from treegenesdb.org (Neale *et al.*, 2017) was extended for this study by including genes expressed in the transcriptomes of Douglas-fir needles during (1) SNC infection (Lind *et al.*, 2022), (2) wasp infection, and (3) cyclic rhythms (Cronn *et al.*, 2017) that were not already present in the previous annotation. These transcriptomes were used to design the probes for this study and therefore including these expressed genes in the annotation would allow for more informative interpretation of the GWAS results. The RNA-Seq reads were assembled *de novo* using TRINITY (v.2.8.5; Grabherr *et al.*, 2011) into 83 829 transcripts with 42 616 cyclic-induced transcripts; 26 261 wasp-induced transcripts; and 14 952 SNC-induced transcripts. The assembled transcripts were mapped to the Douglas-fir reference genome using GMAP (v.2019-03-15) and any previously unannotated genes were appended to the existing annotation, producing a Douglas-fir extended annotation with 94 716 genes. The high number of annotated genes are a result of merging gene annotations from different tissues and assembly sources, and it would be important to verify these gene annotations in the future, particularly those of GWAS top candidate genes. Overlap of genes between case-control groups was tested using the hypergeometric test in R v.4.0.5. Functional annotation of the assembled transcriptome was conducted using ENTAP (Hart *et al.*, 2020). Gene Ontology (GO) enrichment of Biological Process (BP), Molecular Function (MF) and Cellular Component (CC) was conducted using ENTAP annotation TOPGO (v.2.38.1) (Alexa & Rahnenfuhrer, 2024).

Linkage disequilibrium decay estimation

To estimate a proxy related to species-wide linkage disequilibrium (LD), we calculated the correlation in allele frequency among SNPs across all populations using squared Spearman's rank correlation coefficient, ρ^2 (Hill & Robertson, 1968). To calculate background LD, we randomly selected 10 000 SNPs across the genome, then identified all the contigs harboring those 10 000 SNPs and then calculated r^2 among all pairwise combinations of SNPs within each contig. This resulted in us calculating background r^2 within each of 19 095 contigs. The nonlinear decay of r^2 with genomic distance was fitted using Hill and Weir expectation of r^2 between neighboring sites (Hill & Weir, 1988), which is derived for a single population but should give an approximately accurate shape for the expected rate of decay of r^2 with physical distances. We used the equation:

$$(r^2) = (10 + C(2 + C)(11 + C)) \\ \times \left(1 + n(3 + C)(12 + 12C + C^2)(2 + C)(11 + C)\right)$$

where n is sample size, C is the product of the population recombination parameter ($\rho = 4N_e r$) and the distance between SNPs in base pairs as implemented in Remington *et al.* (2001) and

Marroni *et al.* (2011). Nonlinear least squares were used to fit this equation to SNC data using the R package NLS. LD decay or LD half-life was calculated as the point when the observed r^2 between sites decays to less than half the maximum r^2 value. To evaluate the extent of LD around GWAS significant SNPs, we calculated r^2 for all SNPs (neutral and significant) on contigs that contained at least one significant GWAS SNP (for each pool). Using the fitted background LD, we calculated residual LD for all contrasts with the GWAS significant SNPs. Due to the fragmented nature of the Douglas-fir genome, we were only able to assess LD decay within contigs (with a contig N50 of 44 kbp and scaffold N50 of 340 kbp (Neale *et al.*, 2017)) and compare this to the distribution of LD among contigs, which we assume represents the genomic background. This difference in LD decay is biologically relevant for our research question and it is unlikely that contig length would drive spurious associations here. Contig length is more likely to limit our power to detect a decay that extends beyond the bounds of a contig, resulting in a lower-powered analysis. Thus, our interpretation of LD decay patterns around GWAS SNPs is relative to the genomic background and not be interpreted as standalone estimates of LD due to the fragmented nature of the reference genome.

Identifying SNC lineages in Douglas-fir samples

Raw pair-end reads of 132 Douglas-fir samples were aligned to the reference genome of the Swiss needle cast agent (*N. gaeumannii*; GenBank accession no. GCA_002116385) with MINIMAP2 (Li, 2018) using the default parameters. *Nothophaeo-cryptopus gaeumannii* reads were then extracted with SAMTOOLS and biallelic polymorphic loci (SNPs; minimum mapping quality of 30) were called using BCFTOOLS view (Li *et al.*, 2009) and exported in VCF format before being used for lineage assignment.

We designed an assignment procedure to test the most likely origin of the group of unknown isolates as described in Hamelin *et al.* (2022). This procedure consisted of building a Bayesian naïve classifier model for two different classes (i.e. putative SNC genetic lineages (Bennett *et al.*, 2016)) based on k SNP loci and obtaining the probability than an unknown SNC sample to belong to each of these classes. The training set was composed of a set of 100 individuals (66 individuals for lineage 1 and 37 for lineage 2) in which a list of 88 914 haploid SNPs was available. For each sample to test, the classifier was trained with the k SNPs mapped with BCFTOOLS among the list of 88 914 SNPs. Confidence (probability of having a positive when it is a true positive) of the assignment procedure at different k SNP numbers was determined by doing 1000 reassignment iterations with a random sample of one third of the individuals from each SNC lineage. Values of 99.5% confidence in assignment were attained with 8 and 9 SNPs for lineage 1 and 2, respectively. The naïve bayes classifier algorithm was implemented in a custom PYTHON script using the PYTHON package SCIKIT-LEARN 0.24.1 and assuming Multinomial distribution of the data.

Results

GWAS analysis of Douglas-fir response to Swiss needle cast (SNC)

The final dataset for SNC GWAS analysis contained 13 Resistant (R) pools, 55 Tolerant (T) pools and 55 Intolerant (I) pools. 77–85% of sequenced reads across pools mapped to the reference Douglas-fir genome. After SNP calling and filtering for quality, 672 965 SNPs were retained (Fig. S3A). We conducted GWA analysis for SNC tolerant, intolerant and resistant populations and identified 1320 significant SNPs ($P_{\text{adjust}} < 0.05$ FDR corrected) for $\text{SNC}_I \text{ vs } R$ case–control comparison; 1095 significant SNPs ($P_{\text{adjust}} < 0.05$ FDR corrected) for $\text{SNC}_T \text{ vs } R$ case–control comparison; and 182 significant SNPs ($P_{\text{adjust}} < 0.05$ FDR corrected) for $\text{SNC}_I \text{ vs } T$ case–control comparison (Fig. 2a; Table S3). To investigate if SNC tolerant, intolerant and resistant SNPs may have shared genetic architectures, we investigated overlap of significant GWAS SNPs between case–control comparisons. $\text{SNC}_I \text{ vs } R$ and $\text{SNC}_T \text{ vs } R$ analyses had a significant overlap of 84 SNPs (expected overlap = 2.1; $P < 1e-15$), thus we identified 2330 (1320 + 1095 – 84) SNC resistance-associated SNPs. The $\text{SNC}_I \text{ vs } R$ and $\text{SNC}_I \text{ vs } T$ analyses had a significant overlap of three SNPs (expected overlap = 0.4; $P = 5.7e-3$; Fig. 2a). The $\text{SNC}_I \text{ vs } T$ and $\text{SNC}_T \text{ vs } R$ analysis had no overlap in SNPs.

To further investigate the genetic architecture of SNC response phenotypes, we annotated significant GWAS SNPs with the Douglas-fir genome annotation (see Dryad repository). $\text{SNC}_I \text{ vs } R$ SNPs mapped to 614 genes, $\text{SNC}_T \text{ vs } R$ SNPs mapped to 541 genes, and $\text{SNC}_I \text{ vs } T$ SNPs mapped to 82 genes (Fig. 2b;

Table S3). There were no genes overlapping among all three case–control comparisons. Seventy-six genes significantly overlapped between the $\text{SNC}_I \text{ vs } R$ and the $\text{SNC}_T \text{ vs } R$ comparisons ($P < 1e-15$; expected overlap = 10; Fig. 2b; Table S3). Four genes significantly overlapped between the $\text{SNC}_I \text{ vs } R$ and $\text{SNC}_I \text{ vs } T$ comparisons ($P = 0.02$; expected overlap = 1.6) and two genes overlapped between the $\text{SNC}_T \text{ vs } R$ and $\text{SNC}_I \text{ vs } T$ comparisons (not significant $P = 0.14$; expected overlap = 1.3) (Fig. 2b; Table S3). Overall, we found 1073 unique candidate genes underlying resistance to SNC, 76 unique candidate genes underlying tolerance to SNC, and six candidate genes potentially involved in both resistance and tolerance to SNC (Table S3).

Most candidate genes had one significant SNP per gene, but some genes had up to 16 significant SNPs (Figs 2c, S4). The genes with the highest number of significant SNPs were identified from the $\text{SNC}_I \text{ vs } R$ and $\text{SNC}_T \text{ vs } R$ analyses and thus are putatively involved in SNC resistance. Candidate genes for SNC tolerance from the $\text{SNC}_I \text{ vs } T$ analysis had a maximum of three SNPs per gene. Notably, the gene *TPR1* (topless-related protein 1) had 16 significant SNPs; *CYP78A4* (Cytochrome P450 78A4) had 9 significant SNPs; *cyclic_GAZW02100664.1* (gene expressed in circadian rhythm) and *GTG2* (GPCR-type G protein 2) had eight significant SNPs each; three transcripts that were expressed in wasp and SNC-induced libraries (*MSTRG.42441.3_MSTRG.42441*, *wasp_MSTRG.42442.1_MSTRG.42442*, *snc_MSTRG.7080.1_MSTRG.7080*) had seven significant SNPs each; and *RNF8A* (*E3* ubiquitin-protein ligase *rnf8-A*), *PRR* (pentatricopeptide repeat-containing protein) and *DCR* (*BAHD* acyltransferase *DCR*-like) has six significant GWAS SNPs each (Table S3). These genes also had a higher number of significant SNPs compared to the 0.999 quantile of the binomial expectation (Fig. S5).

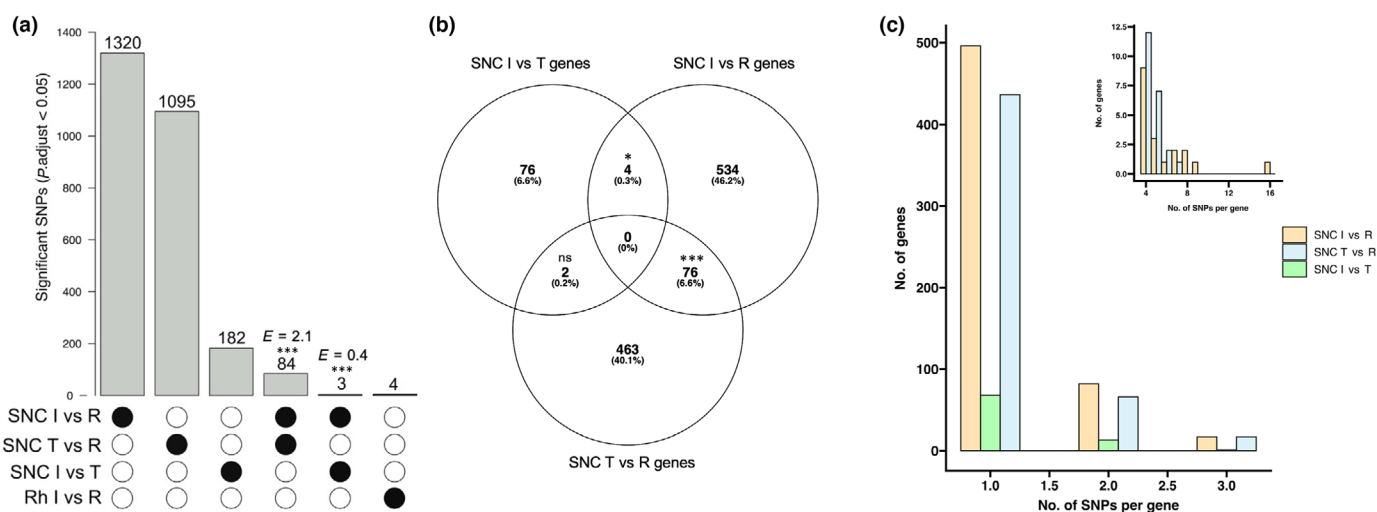


Fig. 2 (a) Number of significantly (false discovery rate adjusted) associated single nucleotide polymorphisms (SNPs) from Swiss needle cast (SNC) and Rhabdocline needle cast genome-wide association studies analysis in coastal Douglas-fir (*Pseudotsuga menziesii* var. *menziesii*) populations. Asterisks indicate significantly greater overlap than expected ($P < 0.005$) by the hypergeometric. Observed overlap indicated below the asterisk and expected overlap indicated above the asterisk. I, disease intolerant; R, disease resistant; T, disease tolerant. (b) Overlap of SNC tolerant, intolerant, and resistant candidate genes. Asterisks denote significant overlaps (by hypergeometric test) and ns denotes nonsignificant overlap. (c) Number of significant SNPs per SNC candidate genes. Inset contains data for four or more SNPs per gene.

Gene ontology enrichment of SNC candidate genes

To functionally annotate genes containing SNC-associated SNPs, we tested GO enrichment of biological processes for the top 100 genes (ranked based on adjusted P -values from the GWAS analysis) for each of three SNC case–control comparisons (Table S3). Relevant enriched GO terms for SNC_I vs R were immune system process, regulation of defense response, jasmonic acid biosynthetic process, response to biotic stimulus, response to chitin and response to wounding (Table S3). Relevant enriched GO terms for SNC_T vs R were immune system process, negative regulation of the ethylene signaling pathway, and stomatal closure and movement (Table S3). Relevant enriched GO terms for SNC_I vs T were immune system process, flavonoid, phenol, terpenoid, lignin, and antibiotic metabolic processes (Table S3). Candidate genes annotated with defense or immune response functions were: TPR1, GTG2, HIR1, OPR2, RD19B, PAD4 and CYP78A4 from the SNC_I vs R comparison; ETR2, LOX, PER21, PRR and SDH from the SNC_T vs R comparison; and FMO1, RD19B and At5g63020 (a predicted R gene) from the SNC_I vs T comparison (Table S3).

Linkage disequilibrium of significant SNC SNPs

Natural selection on beneficial mutations generates LD with physically linked neutral alleles. To investigate if significant SNC GWA SNPs were under selection in Douglas-fir, we used LD as proxy for signature of selection. We defined LD decay as the point when the observed r^2 between SNPs decays to less than half the maximum r^2 value. SNC resistance and tolerance-associated SNPs had significantly higher LD than background LD decay distance for randomly chosen regions in the genome, calculated using all SNPs across a random subset of 19 095 contigs (P -value < $2.2\text{e-}16$ background vs SNC_I vs R; P -value = $1.207\text{e-}11$ background vs SNC_T vs R; P -value = $1.208\text{e-}06$ background vs SNC_I vs T; Fig. 3a). The background LD decay distance was 224 bp (Fig. S6). Compared to the background, the LD decay distance of SNC_I vs R SNPs was the largest at 1260 bp, followed by SNC_T vs R SNPs at 762 bp, and the SNC_I vs T SNPs at 450 bp (Fig. S6). Thus, SNC resistance-associated SNPs exhibited stronger LD than SNC tolerance-associated SNPs, which is suggestive of stronger selection on SNC resistance than tolerance. Natural selection on both SNC tolerance and resistance-associated SNPs would be expected to result in genetic hitchhiking of neutral alleles on the same contig, generating apparent associations with phenotype at these loci. To look for this signature, we also analyzed the relationship between the number of significant SNC-associated SNPs found per gene and pattern of LD across that gene (Fig. 3b–d). To represent the amount of LD across a gene relative to the background expectation, for each pairwise combination of SNPs we represented their observed LD as a residual relative to the LD decay model that was fit to the background SNPs and took the average across these residuals. As expected, due to genetic hitchhiking hypothesis, we found a significant positive relationship between the number of SNPs associated with SNC resistance in a gene and the average residual LD

across those genes for candidate genes from the SNC T vs R comparison (P -value = 0.005, correlation = 0.12, Fig. 3d). This relationship was not significant for genes from the SNC I vs R comparison or the SNC I vs T comparison (Fig. 3b,c).

GWAS analysis of Douglas-fir response to Rhabdocline needle cast

The final RNC GWAS analysis had five Resistant (R) and five Intolerant (I) pools. 80–84% reads from RNC pools mapped to the reference Douglas-fir genome. 1016 287 SNPs were retained after filtering across five Intolerant (I) and five Resistant (R) pools (Fig. S3B). We conducted GWA analysis for RNC and identified four significant SNPs ($P_{\text{adjust}} < 0.05$) for RNC_I vs R case–control comparison (Fig. 2a; Table S3). The RNC significant SNPs had no overlap with SNC significant SNPs. We estimated the correlation of the allele frequencies of the four SNPs in our dataset as a proxy for LD and found three SNPs are in a cluster of high LD with each other (Spearman's $\rho > 0.6$; Fig. 4a). We annotated the four RNC significant SNPs and only one mapped to two genes (not fully overlapping) located on opposite strands, while the other three SNPs were intergenic. On the – strand was Eukaryotic Release Factor 1 (ERF1) and on the + strand was the Eukaryotic Release Factor 105 (ERF105) (Table S3).

SNC lineage identification

To identify SNC lineages infecting Douglas-fir in our sampling sites we mapped sequenced reads to the *N. gaeumannii* genome. For the SNC samples, an average of 0.05% (SD = 0.012) of the sequenced reads could be mapped on the *N. gaeumannii* samples. Interestingly, similar proportion of reads could also be mapped on *N. gaeumannii* genome for *Rhabdocline* samples, indicating that *N. gaeumannii* biomass was likely present in *Rhabdocline*-infected needles. One to 4180 SNPs could be mapped, depending on the sample tested (median = 29 SNPs). A total of 117 samples (88.6%) analyzed had the minimum number of SNPs required (≥ 8) to obtain assignments with $\geq 99.5\%$ confidence. This resulted in 61 samples assigned to lineage 1 and 56 samples to lineage 2 (Table S4). Warmer and wetter sites of the Oregon coast were dominated by lineage 2, while lineage 1 was more abundant more eastern and northern sites (Table 1). This pattern matched previous observations made on the geographical distribution and ecological preference of the two SNC genetic lineages (Bennett *et al.*, 2016, 2019).

Discussion

The eco-evolutionary dynamic of climate change and plant pathogens has increased the severity of disease in agricultural and wild plant communities (Garrett *et al.*, 2006). However, our limited understanding of the genetic, adaptive, and mechanistic patterns of plant–pathogen interactions impedes critical management and conservation decisions. This makes empirical studies delineating the genetic basis of disease resistance crucial.

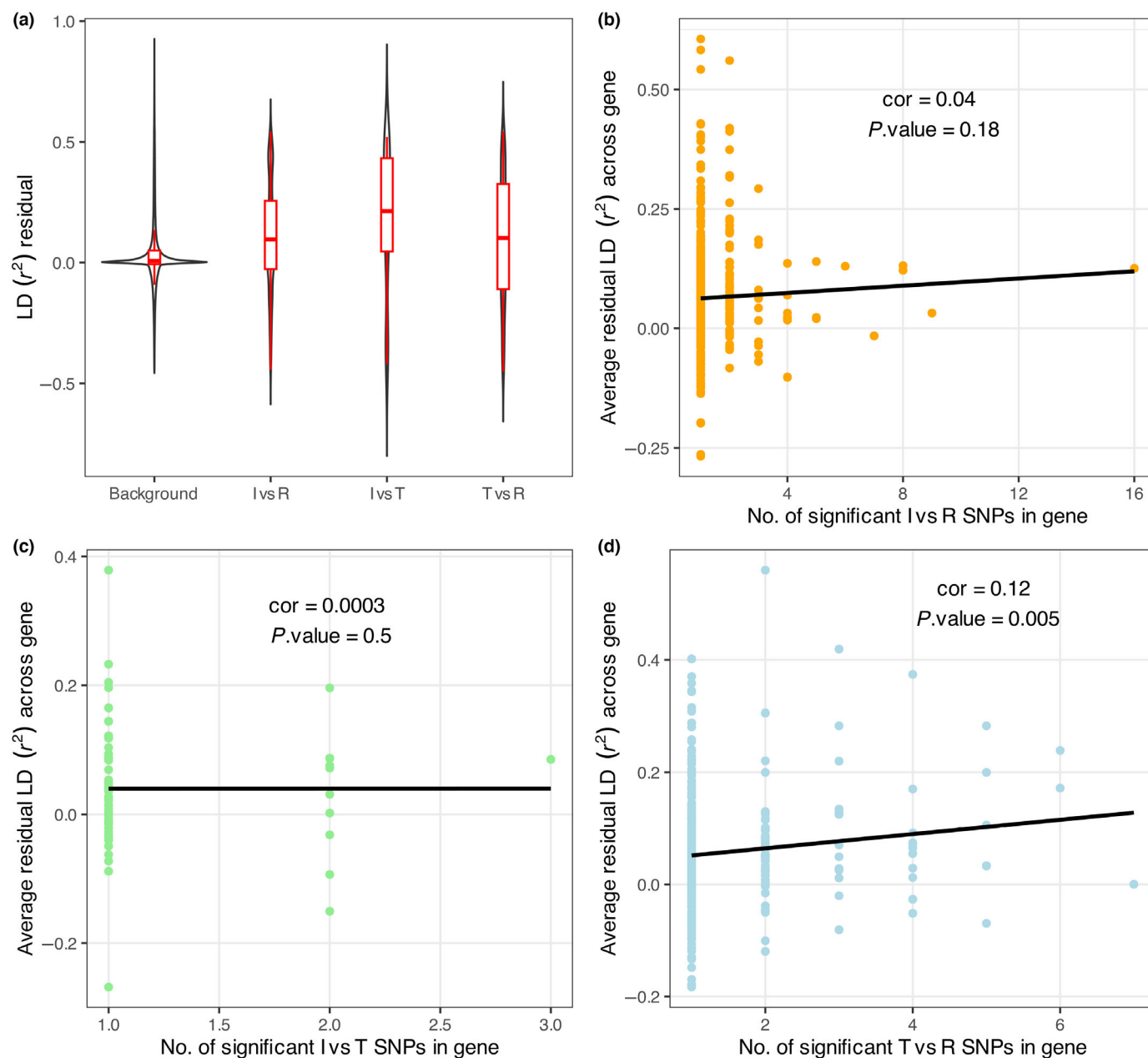


Fig. 3 Decay in linkage disequilibrium (LD) around single nucleotide polymorphisms (SNPs) associated with Swiss needle cast (SNC) resistance, tolerance, and intolerance in coastal Douglas-fir (*Pseudotsuga menziesii* var. *menziesii*) populations. A model was fit to genome-wide data to describe the decay in LD with physical distance (LD inferred from r^2 in allele frequencies across populations), with residuals indicating the relative increase/decrease in the rate of LD decay around a target SNP of interest. (a) Linkage disequilibrium residuals around SNC-associated SNPs, compared to randomly chosen loci from the genomic background. Horizontal line in boxplot represents median and whiskers represent maximum and minimum values, excluding outliers. SNPs from all three SNC groups have significantly greater LD than the background ($P < 0.000001$). (b–d) Relationship between the number of significant SNPs found per gene vs average LD across the gene investigated using a linear regression. Pearson correlation value and P -value significance is shown.

Tolerance and resistance represent two major plant defense mechanisms (Baucom & De Roode, 2011). While pathogen resistance has been extensively studied, tolerance is less understood in comparison because disease resistance is considered evolutionarily more important (Pagán & García-Arenal, 2018). By contrast, it has been hypothesized that tolerance and not resistance is the primary defense mechanism of Douglas-fir trees

against SNC because *N. gaeumannii* is an endophyte (Temel *et al.*, 2004, 2005). However, we have only a limited understanding of the genetic basis of tolerance and resistance to SNC, even though this disease has had a major impact on the forestry economy of the Pacific Northwest, and climate change is increasing this impact (Shaw *et al.*, 2021). We found that both resistance and tolerance to SNC had complex genetic architectures

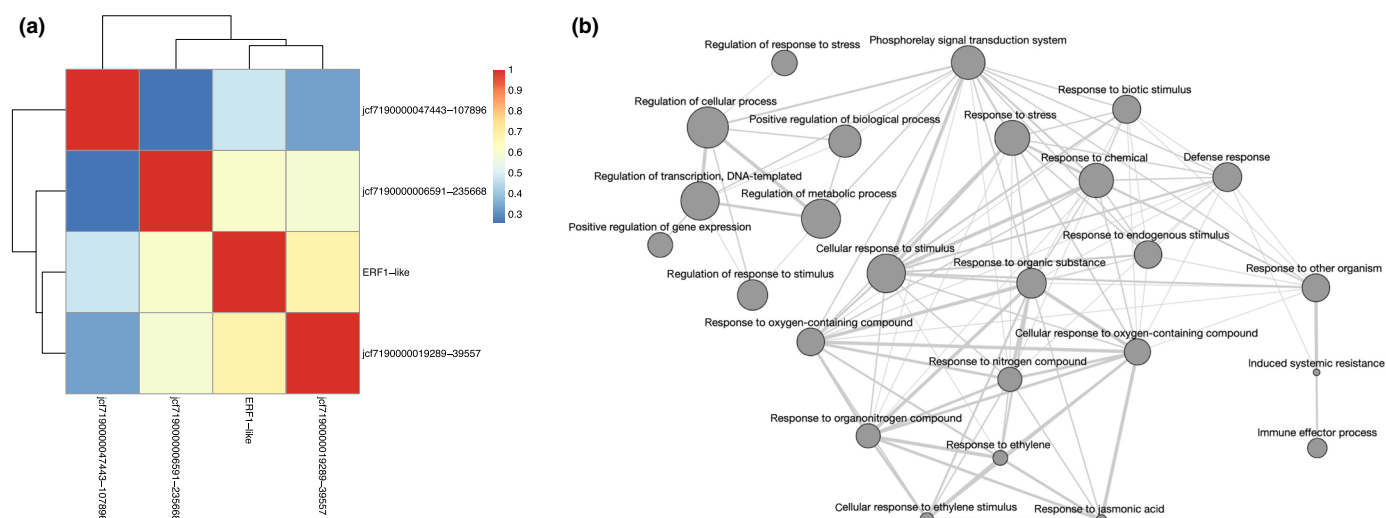


Fig. 4 Patterns of linkage disequilibrium and Gene Ontology (GO) terms associated with Rhabdocline needle cast (RNC) resistant single nucleotide polymorphisms (SNPs) in coastal Douglas-fir (*Pseudotsuga menziesii* var. *menziesii*) populations. (a) Spearman's rho correlation coefficients of allele frequencies of four RNC significant SNPs, one of which maps to the ERF1 gene. Heatmap color scale depicts the range of Spearman's rho coefficients among SNPs. Tree topology in heatmap is calculated by hierarchical clustering of rho coefficients. (b) Gene Ontology network of the biological processes associated with the ERF1 gene. Highly similar GO terms are linked by edges, where line width indicates level of similarity. The size of the circle corresponds to the frequency of GO term in the GO database, with large circles representing more general terms.

involving hundreds of SNPs (and many genes), which may reflect the complex pathology of this disease (Stone, 2018; Montwé *et al.*, 2021). Plant disease resistance is a quantitative trait (Young, 1996); therefore, our discovery of many candidate genes associated with SNC resistance is not surprising. Contrary to

previous studies that suggest that disease tolerance involves few genes (Pagán & García-Arenal, 2018), we identified 82 candidate genes associated with SNC tolerance (SNC I vs T). This suggests that tolerance to SNC in Douglas-fir, and tolerance perhaps more broadly in plants, may be much more complex genetically than

Table 1 Candidate genes for Swiss needle cast resistance and tolerance and Rhabdocline needle cast resistance in coastal Douglas-fir (*Pseudotsuga menziesii* var. *menziesii*) tree populations identified using genome-wide association analysis.

	Gene name	Function	Reference
Swiss needle cast resistance	<i>AS1-like</i>	Negatively regulates inducible resistance against pathogens by binding to promoters of the jasmonic acid pathway	Nurmberg <i>et al.</i> (2007)
	<i>GTG2</i>	G-protein-coupled receptor for abscisic acid. Regulates stomatal closure, restricting pathogen invasion	Pandey <i>et al.</i> (2009); Zhang <i>et al.</i> (2012)
	<i>PRR</i>	Activates immune response after detecting pathogen-associated molecular patterns	Wang & Chai (2020)
	<i>PAD4</i>	Plays a role in salicylic acid-dependent plant defense against pathogens	Jirage <i>et al.</i> (1999)
	<i>PER21</i>	Involved in plant defense responses against pathogenic fungi	Mir <i>et al.</i> (2015)
	<i>SDH</i>	Regulates plant defense to fungi in potatoes via the salicylic acid pathway	Zhang <i>et al.</i> (2020)
	<i>DCR-like</i>	Plays a key role in the formation of cutin, which that acts as a physical defense barrier against invading fungal pathogens	Panikashvili <i>et al.</i> (2009); Serrano <i>et al.</i> (2014)
	<i>At1g67720</i>	A probable Resistance (R) geneLRR receptor-like serine/threonine-protein kinase	–
	<i>TPR1</i>	Activates TIR-NB-LRR R protein-mediated immune responses	Zhu <i>et al.</i> (2010)
	<i>ETR2</i>	Ethylene receptor. Ethylene mediates pathogen response	Sakai <i>et al.</i> (1998)
Swiss needle cast tolerance	<i>LOX</i>	Involved in defense against pathogens	Kolomiets <i>et al.</i> (2000)
	<i>FMO1</i>	Critical for systemic acquired resistance in plants	Mishina & Zeier (2006)
	<i>RD19B</i>	Required for bacterial disease resistance activation	Bernoux <i>et al.</i> (2008)
	<i>At5g63020</i>	Predicted R gene	–
	<i>COMT</i>	Involved in lignin biosynthesis	Ma & Xu (2008)
Rhabdocline needle cast resistance	<i>ERF1</i>	Transcription factor downstream of ethylene and jasmonate signaling pathways that regulates disease progression	Lorenzo <i>et al.</i> (2003)

previously thought, where selection can target multiple points in (perhaps multiple) physiological pathways that can lead to pathogenic tolerance.

Disease tolerance and resistance mechanisms in plants are known to coexist and evolve simultaneously (Restif & Koella, 2004). While most plant defense evolutionary models assume the two mechanisms to be independent, it has been shown that they can be co-dependent or correlated (Howick & Lazzaro, 2017). We found small overlap of only three SNC resistant and tolerance-associated SNPs, suggesting that the genetic bases of tolerance and resistance to SNC in Douglas-fir are distinct. This was echoed in only six candidate genes being associated with both SNC resistance and tolerance. This suggested that SNC tolerance and defense have distinct and nonoverlapping genetic architectures. Nonoverlapping genetic architectures of these two SNC defense mechanisms in Douglas-fir may allow them to evolve independently and reduce constraints imposed by genetic trade-offs (Howick & Lazzaro, 2017). One of the six overlapping genes was the cysteine protease RD19B that is known to play a role in pathogen resistance in *Arabidopsis thaliana* (Bernoux *et al.*, 2008). Given that each of these pairs of contrasts involves repeated use of the same pool of individuals (e.g. both I vs R and T vs R involve comparison with the R strain), this limited overlap is particularly noteworthy as more overlap might be expected given the nonindependence of the comparisons.

Plants have evolved constitutive and induced immunity for defense against pests and pathogens (Freeman & Beattie, 2008). Constitutive defenses consist of structural barriers such as waxy cuticles and cell wall. We found the lignin biosynthesis gene COMT to be associated with SNC resistance, indicating that lignin biosynthesis might be involved in resistance to *N. gaumannii* (Ma & Xu, 2008). Lignin deposition can act as a physical barrier restricting pathogen growth as it is recalcitrant to degradation (Lee *et al.*, 2019). By contrast, induced defenses in plants involve the production of chemicals, enzymes that degrade pathogen cells (Freeman & Beattie, 2008). There are two categories of induced resistance (1) Systemic acquired resistance (SAR), which is a salicylic acid-dependent process (Lefevre *et al.*, 2020); (2) Induced systemic resistance (ISR), which is mediated by the phytohormones ethylene and jasmonate (Hammerschmidt, 1999). Plants produce phytohormones to respond to environmental stressors such as fungal pathogens, rapidly and specifically. Both jasmonic acid and ethylene signaling pathways were enriched in genes associated with SNC resistance (Miller *et al.*, 2017). By contrast, SNC tolerance genes were enriched for flavonoid, phenol, terpenoid, lignin metabolic process and antibiotic metabolic process. Flavonoids, phenols, and terpenes are secondary metabolites that can function as antibiotics in plants (Falcone Ferreyra *et al.*, 2012; Sharma *et al.*, 2017; Tuladhar *et al.*, 2021). Overall, we find that plant phytohormones and structural barriers play a larger role in SNC resistance and secondary metabolites play a larger role in SNC tolerance in Douglas-fir. It must be noted that our GWAS analysis did not have the power to differentiate between the genetic basis of Douglas-fir's response to two lineages of SNC identified in our dataset. This would be an avenue worth exploring in future

studies, especially as SNC lineage 1 is known to be more aggressive than lineage 2 (Bennett *et al.*, 2016, 2019).

This study identified several promising candidate genes for disease resistance and tolerance (Table 1). One of the most exciting candidate genes for SNC resistance was the AS1-like gene, which is a transcription factor that negatively regulates inducible resistance against pathogens by binding to promoters of the jasmonic acid pathway (Nurmberg *et al.*, 2007). Loss of function mutations of AS1 were found to increase resistance against necrotrophic fungi in *A. thaliana* (Nurmberg *et al.*, 2007). This suggests that its function is evolutionarily conserved in plants spanning a 125 million years ago of divergence. Another important candidate gene for SNC resistance was GTG2, a G-protein-coupled receptor for abscisic acid (Pandey *et al.*, 2009). G-proteins are known to play a role in plant immunity by regulating stomatal closure, restricting pathogen invasion (Zhang *et al.*, 2012). Abscisic acid is one of the best studied regulators of stomatal closure (Wang *et al.*, 2011) and regulation of stomatal closure was an enriched GO term for SNC resistance genes. Closing the stomata may have evolved as a constitutive defense response that resists SNC by preventing *N. gaumannii* from entering Douglas-fir needles. Other important candidates for SNC resistance were PRR, a receptor that activates immune response after detecting pathogen-associated molecular patterns (Wang & Chai, 2020); PAD4, which plays a role in salicylic acid-dependent plant defense against pathogens (Jirage *et al.*, 1999); PER21, a member of peroxidase family that are evolutionarily conserved and involved in plant defense responses against pathogenic fungi (Mir *et al.*, 2015); SDH, a succinate dehydrogenase that regulates plant defense to fungi in potatoes via the salicylic acid pathway (Zhang *et al.*, 2020); a DCR-like gene that plays a key role in the formation of cutin, which is a key component of the plant cuticle that acts as a physical defense barrier against invading fungal pathogens (Panikashvili *et al.*, 2009; Serrano *et al.*, 2014); and a probable Resistance (R) gene: the LRR receptor-like serine/threonine-protein kinase (Atlg67720). All this evidence points to a strong immune response from Douglas-fir to *N. gaumannii* infection. This contradicts previous thinking that the endophytic nature of *N. gaumannii* prevents it from triggering host immunity compared to necrotrophic fungal pathogens.

Pathogens impose strong selection pressure on their hosts. Positive selection occurs when an allele favored by natural selection increases in frequency in the population. Due to genetic hitchhiking, neighboring linked neutral alleles also increase in frequency, reducing nearby variation, which results in selective sweeps (Maynard Smith & Haigh, 1974; Barton, 2000). Such signatures of positive selection can be detected by searching for regions of reduced variation or elevated LD patterns introduced by selective sweeps across the genome (Nielsen, 2005). While we lost haplotype information with our pool-seq datasets, we use the correlation of allele frequencies across populations between loci as a proxy for LD. This method is highly correlated to haplotype-derived estimates (Lucek & Willi, 2021). We found that LD among SNC tolerance and resistance-associated SNPs was significantly higher than background LD (Fig. 3a). Additionally, LD decay distance on contigs with SNC resistance-associated SNPs was fivefold higher than from random background contigs, and

LD decay on contigs with SNC tolerance-associated SNPs was twofold higher than random background contigs (Fig. S6). Together, patterns of LD suggest that SNC tolerance and resistance-associated SNPs are experiencing positive selection in Douglas-fir and that selection is stronger on resistance-associated SNPs than the tolerance-associated SNPs. The other alternative of course is that high LD is driven by low recombination or other demographic factors and not selection (Ptak *et al.*, 2004).

Genetic hitchhiking is the increase in allele frequency of neutral/deleterious SNPs due to physical linkage to a SNP under selection (Fay & Wu, 2000; Mitchell-Olds *et al.*, 2007). Thus, genetic hitchhiking can be an indicator of the strength of natural selection (Charlesworth *et al.*, 1997) and this assumption has formed the basis of tests for adaptation (Yeaman *et al.*, 2016). However, such tests are limited in power to cannot detect selection in genes with few SNPs. We found that candidate genes for SNC resistance phenotypes had some of the highest number of significant SNPs per gene, exceeding expectation under the binomial distribution that accounts for the total number of SNPs per gene (Fig. S5). This suggests that at least one causal SNC resistance variant (which is unknown to us) is under strong natural selection. To estimate the extent of genetic hitchhiking around SNC resistant/tolerant SNPs, we calculated the LD between SNC-associated SNPs and all other SNPs on the same contigs and estimated the rate of LD decay with physical distance. SNC resistance and tolerance-associated SNPs had higher LD than background levels (Fig. 3a). We also found a positive relationship between number of significant SNPs per genes and the landscape of LD decay around that gene, suggesting that selection on causal SNC resistance-associated variants causes elevated LD (Fig. 3d). This relationship did not hold for SNC tolerance-associated SNPs. This strong relationship between LD and SNP number also implies that the true number of causal variants underlying SNC resistance is lower than what we found. Of note was the gene TPR1 that contains 16 significant SNPs. This gene has been shown to activate TIR-NB-LRR R protein-mediated immune responses by repressing its negative regulators in *A. thaliana* (Zhu *et al.*, 2010). Of 16 significant SNPs in TPR1, one SNP was synonymous and the other 15 SNPs were in introns (see Supplementary Data on Dryad). However, this gene also contained 52 other SNPs (that were not GWAS outliers) of which 11 were nonsynonymous SNPs, three were synonymous and one SNP resulted in a premature stop codon. Disease resistance genes are some of the fastest evolving genes and the high number of SNPs in TPR1 may be indicative of rapid evolution. Furthermore, premature stop codons are thought to play a role in regulating R proteins (Parker *et al.*, 2021). The GTG2, PRR, and DCR-like genes discussed above had six or more outlier SNPs each. While likely driven in part by hitchhiking with strong selection, this high number of significant SNPs in SNC resistance genes may also represent selection on multiple causal variants, as the result of the plant–pathogen arms race that requires plant R genes to constantly evolve to keep up with the evolutionary trajectory of the pathogen (Yang *et al.*, 2013).

The most strongly associated candidate gene for RNC resistance was ERF1, a member of the ERF/AP2 transcription factor family. ERF1 acts downstream of two major plant immunity pathways (ethylene and jasmonate signaling, Fig. 4b), regulating pathogen response genes that inhibit disease progression (Lorenzo *et al.*, 2003). It is possible (but unlikely) that RNC resistance in Douglas-fir involves only one large effect gene. However, it is more likely that our statistical power to detect more RNC resistance-associated SNPs was limited by the few individuals that were sampled for this GWAS comparison. Interestingly, the ERF1 gene was found to be locally adapted to summer heat moisture and Hargreaves climate moisture deficit environmental variables in natural populations of coastal Douglas-fir (Lind *et al.*, 2023). This is striking as *R. pseudotsugae* spore release is dependent on moisture available through high humidity, dew, or rainfall (Wilhelmi *et al.*, 2021). It also implies that climate change will impact the ability of Douglas-fir trees to respond to RNC.

A limitation of our study is that we pooled continuous disease phenotypes into binary case–control groups. This mostly likely decreased our power to detect smaller effect loci and resulted in loss of haplotype information. However, the trade-off between sequencing costs and DNA pooling allowed us to include more Douglas-fir populations and hence include more genetic variation in our GWAS analysis. Our experimental approach leveraged samples from an extensive field experiment and had the advantage of studying host responses in multiple populations, on multiple sites, in a large common garden under natural conditions, with naturally occurring infection. While a controlled glasshouse experiment with controlled infections would make the GWAS less noisy, field experiments provide a more realistic picture of the multifaceted selection pressures that trees face in nature. Another potential limitation in our study may arise from the lack of a chromosome-scale reference genome assembly. It is possible that multiple contigs with strong association signals are actually tightly linked, so that the hitchhiking effect we observed within contigs is also driving some noncausal associations in other contigs. However, it is difficult to assess this without a chromosome-scale reference genome to explore any patterning in the distribution of our associated loci across chromosomes. Because pool-seq approaches are unable to resolve haplotypes, our estimation of LD is constrained to among-population components that are observable as correlations in allele frequency across populations. Thus, some of our analyses related to LD might be less sensitive than analyses based on individual haplotypes.

In conclusion, our study sheds light on the complex genetic architectures of tolerance and resistance to the little understood needle cast diseases SNC and RNC. We find that genetic variation associated with disease resistance is under strong selection and that disease tolerance plays an important role in tree immunity. The SNP array that we designed using the SNPs identified in this study pave the way for improved genomics-informed selection and breeding approached in forestry management and conservation of Douglas-fir trees.

Acknowledgements

We would like to acknowledge the traditional territories of the peoples of the Treaty 7 region in Southern Alberta and the traditional, ancestral, unceded territory of the Musqueam First Nation where this research was conducted. The CoAdapTree project is funded by Genome Canada (241REF; Co-Project Leaders SNA, SY and RH), with co-funding from Genome BC and 16 other sponsors (<http://coadapttree.forestry.ubc.ca/sponsors/>), including Genome Alberta, Génome Québec, the BC Ministry of Forests, Alberta Innovates Bio Solutions, Vernon Seed Orchard Company, University of Alberta, University of British Columbia, Digital Research Alliance of Canada, Mosaic Forest Management, and Western Forest Products. We would also like acknowledge funding from NSERC (SY, SNA), Alberta Innovates, Digital Research Alliance of Canada; and the US Forest Service. We thank Centre d'expertise et de services Génome Québec for sequencing service.








Competing interests

None declared.

Author contributions

PS conducted the main analyses and interpretation, and wrote and revised the manuscript. JBS conceived the study and established the study design. BML contributed to the bioinformatics analysis. RC contributed to the sampling and DNA extraction. NPW contributed to the sampling and phenotyping. NF contributed to the SNC lineage analysis. ML designed the pool-seq probes and modified CMH test. DOV contributed to the library construction. RCH and SNA conceived the study and acquired the funding. DCS contributed to the sampling and phenotyping design. SY conceived the study, acquired the funding, and contributed to the sampling design and CMH test. All authors approved the final version of the manuscript.

ORCID

Sally N. Aitken  <https://orcid.org/0000-0002-2228-3625>
 Richard Cronn  <https://orcid.org/0000-0001-5342-3494>
 Nicolas Feau  <https://orcid.org/0000-0001-5925-9867>
 Richard C. Hamelin  <https://orcid.org/0000-0003-4006-532X>
 Brandon M. Lind  <https://orcid.org/0000-0002-8560-5417>
 Mengmeng Lu  <https://orcid.org/0000-0001-5023-3759>
 Pooja Singh  <https://orcid.org/0000-0001-6576-400X>
 Sam Yeaman  <https://orcid.org/0000-0002-1706-8699>

Data availability

All analysis code is available on GitHub (<https://github.com/CoAdapTree> and https://github.com/poojasingh09/2022_Singh_et_al_GWAS_SNC). Main result files are available on Dryad (doi: [10.5061/dryad.jdfn2z3dp](https://doi.org/10.5061/dryad.jdfn2z3dp)). All raw sequencing data

has been deposited to the NCBI SRA (BioProject PRJNA867661).

References

- Alexa A, Rahnenfuhrer J. 2024. *TOPGO: enrichment analysis for gene ontology*. R package v.2.56.0.
- Barton NH. 2000. Genetic hitchhiking. *Philosophical Transactions of the Royal Society of London. Series B: Biological Sciences* 355: 1553–1562.
- Baucom RS, De Roode JC. 2011. Ecological immunology and tolerance in plants and animals. *Functional Ecology* 25: 18–28.
- Bennett P, Stone J, Stenlid J, Oliva J, Menkis A. 2016. Assessments of population structure, diversity, and phylogeography of the Swiss Needle Cast fungus (*Phaeocryptopus gaeumannii*) in the U.S. Pacific Northwest. *Forests* 7: 14.
- Bennett PI, Stone JK, Patrick Bennett CI. 2019. Environmental variables associated with *Nothophaeocryptopus gaeumannii* population structure and Swiss needle cast severity in Western Oregon and Washington. *Ecology and Evolution* 9: 11379–11394.
- Bergot M, Cloppet E, Pérarnaud V, Déqué M, Marçais B, Desprez-Loustau M. 2004. Simulation of potential range expansion of oak disease caused by *Phytophthora cinnamomi* under climate change. *Global Change Biology* 10: 1539–1552.
- Bernoux M, Timmers T, Jauneau A, Brière C, de Wit PJGM, Marco Y, Deslandes L. 2008. RD19, an Arabidopsis cysteine protease required for RRS1-R-mediated resistance, is relocalized to the nucleus by the *Ralstonia solanacearum* PopP2 effector. *Plant Cell* 20: 2252–2264.
- Black BA, Shaw DC, Stone JK. 2010. Impacts of Swiss needle cast on overstory Douglas-fir forests of the western Oregon Coast Range. *Forest Ecology and Management* 259: 1673–1680.
- Boyce JS. 1940. A needle cast of Douglas Fir associated with *Adelopus gaeumannii*. *Phytopathology* 30: 649–655.
- Brandt RW. 1960. *The rhabdocone needle cast of Douglas fir*. Syracuse, NY, USA: State University College of Forestry.
- Capitano B. 1999. *The infection and colonization of Douglas-fir by Phaeocryptopus gaeumannii*. MSc thesis, Department of Botany and Plant Pathology, Oregon State University, Corvallis, OR, USA.
- Charlesworth B, Nordborg M, Charlesworth D. 1997. The effects of local selection, balanced polymorphism and background selection on equilibrium patterns of genetic diversity in subdivided populations. *Genetical Research* 70: 155–174.
- Chastagner GA, Byther RS, Riley KL. 1990. Maturation of apothecia and control of Rhabdocone needlecast on Douglas-fir in western Washington. In: Merrill W, Ostry ME, eds. *Proceedings of conference on recent research on foliage diseases*. Carlisle, PA, USA: USDA Forest Service, 87–92.
- Chastagner GA. 2001. Susceptibility of intermountain Douglas-Fir to rhabdocone needle cast when grown in the Pacific Northwest. *Plant Health Progress* 2: 2.
- Chen S, Zhou Y, Chen Y, Gu J. 2018. FASTP: an ultra-fast all-in-one FASTQ preprocessor. *Bioinformatics* 34: i884–i890.
- Croll D, McDonald BA. 2017. The genetic basis of local adaptation for pathogenic fungi in agricultural ecosystems. *Molecular Ecology* 26: 2027–2040.
- Cronn R, Dolan PC, Jogdeo S, Wegrzyn JL, Neale DB, St. Clair JB, Denver DR. 2017. Transcription through the eye of a needle: daily and annual cyclic gene expression variation in Douglas-fir needles. *BMC Genomics* 18: 558.
- Evans N, Baierl A, Semenov MA, Gladders P, Fitt BDL. 2008. Range and severity of a plant disease increased by global warming. *Journal of the Royal Society Interface* 5: 525–531.
- Falcone Ferreyra ML, Rius S, Casati P. 2012. Flavonoids: biosynthesis, biological functions, and biotechnological applications. *Frontiers in Plant Science* 3: 222.
- Fay JC, Wu CI. 2000. Hitchhiking under positive Darwinian selection. *Genetics* 155: 1405–1413.
- Freeman B, Beattie G. 2008. An overview of plant defenses against pathogens and herbivores. *The Plant Health Instructor* 8: 226–301.

- Garrett KA, Dendy SP, Frank EE, Rouse MN, Travers SE. 2006. Climate change effects on plant disease: genomes to ecosystems. *Annual Review of Phytopathology* 44: 489–509.
- Grabherr MG, Haas BJ, Yassour M, Levin JZ, Thompson DA, Amit I, Adiconis X, Fan L, Raychowdhury R, Zeng Q *et al.* 2011. Full-length transcriptome assembly from RNA-Seq data without a reference genome. *Nature Biotechnology* 29: 644–652.
- Hamelin RC, Bilodeau GJ, Heinzlmann R, Hrywkiw K, Capron A, Dort E, Dale AL, Giroux E, Kus S, Carleson NC *et al.* 2022. Genomic biosurveillance detects a sexual hybrid in the sudden oak death pathogen. *Communications Biology* 5: 477.
- Hammerschmidt R. 1999. Induced disease resistance: how do induced plants stop pathogens? *Physiological and Molecular Plant Pathology* 55: 77–84.
- Hansen EM, Stone JK, Capitano BR, Rosso P, Sutton W, Winton L, Kanaskie A, McWilliams MG. 2000. Incidence and impact of Swiss needle cast in forest plantations of Douglas-fir in Coastal Oregon. *Plant Disease* 84: 773–778.
- Hart AJ, Ginzburg S, Xu M, Fisher CR, Rahmatpour N, Mitton JB, Paul R, Wegryn JL. 2020. EN-TAP: bringing faster and smarter functional annotation to non-model eukaryotic transcriptomes. *Molecular Ecology Resources* 20: 591–604.
- Herpin-Saunier NYH, Sambaraju KR, Yin X, Feau N, Zeglen S, Ritokova G, Omdal D, Côté C, Hamelin RC. 2022. Genetic lineage distribution modeling to predict epidemics of a conifer disease. *Frontiers in Forests and Global Change* 4: 756678.
- Hill WG, Robertson A. 1968. Linkage disequilibrium in finite populations. *Theoretical and Applied Genetics* 38: 226–231.
- Hill WG, Weir BS. 1988. Variances and covariances of squared linkage disequilibria in finite populations. *Theoretical Population Biology* 33: 54–78.
- Howick VM, Lazzaro BP. 2017. The genetic architecture of defence as resistance to and tolerance of bacterial infection in *Drosophila melanogaster*. *Molecular Ecology* 26: 1533–1546.
- Jirage D, Tootle TL, Reuber TL, Frost LN, Feys BJ, Parker JE, Ausubel FM, Glazebrook J. 1999. *Arabidopsis thaliana* PAD4 encodes a lipase-like gene that is important for salicylic acid signaling. *Proceedings of the National Academy of Sciences, USA* 96: 13583–13588.
- Juroszek P, Racca P, Link S, Farhumand J, Kleinhenz B. 2020. Overview on the review articles published during the past 30 years relating to the potential climate change effects on plant pathogens and crop disease risks. *Plant Pathology* 69: 179–193.
- Koboldt DC, Zhang Q, Larson DE, Shen D, McLellan MD, Lin L, Miller CA, Mardis ER, Ding L, Wilson RK. 2012. VarScan 2: somatic mutation and copy number alteration discovery in cancer by exome sequencing. *Genome Research* 22: 568–576.
- Kolomiets MV, Chen H, Gladon RJ, Braun EJ, Hannapel DJ. 2000. A leaf lipoxygenase of potato induced specifically by pathogen infection. *Plant Physiology* 124: 1121–1130.
- Kurkela T. 1981. *Growth reduction in Douglas fir caused by Rhabdochline needle cast*. Helsinki, Finland: Finnish Forest Research Institute.
- Lee EH, Beedlow PA, Waschmann RS, Tingey DT, Cline S, Bollman M, Wickham C, Carlile C. 2017. Regional patterns of increasing Swiss needle cast impacts on Douglas-fir growth with warming temperatures. *Ecology and Evolution* 7: 11167–11196.
- Lee M-H, Jeon HS, Kim SH, Chung JH, Roppolo D, Lee H-J, Cho HJ, Tobimatsu Y, Ralph J, Park OK. 2019. Lignin-based barrier restricts pathogens to the infection site and confers resistance in plants. *EMBO Journal* 38: e101948.
- Lefevre H, Bauters L, Gheysen G. 2020. Salicylic acid biosynthesis in plants. *Frontiers in Plant Science* 11: 338.
- Li H. 2018. MINIMAP2: pairwise alignment for nucleotide sequences. *Bioinformatics* 34: 3094–3100.
- Li H, Durbin R. 2009. Fast and accurate short read alignment with Burrows-Wheeler transform. *Bioinformatics* 25: 1754–1760.
- Li H, Handsaker B, Wysoker A, Fennell T, Ruan J, Homer N, Marth G, Abecasis G, Durbin R. 2009. The Sequence Alignment/Map format and SAMTOOLS. *Bioinformatics* 25: 2078–2079.
- Lind B. 2022. [WWW document] URL https://GitHub.com/CoAdapTree/varsan_pipeline [accessed 16 May 2024].
- Lind B. 2023. [WWW document] URL https://GitHub.com/brandonlind/cmh_test [accessed 16 May 2024].
- Lind BM, Candido-Ribeiro R, Singh P, Lu M, Obrecht Vidakovic D, Booker TR, Whitlock MC, Yeaman S, Isabel N, Aitken SN. 2023. How useful is genomic data for predicting maladaptation to future climate? *Global Change Biology* 30: e17227.
- Lind BM, Lu M, Obrecht Vidakovic D, Singh P, Booker TR, Aitken SN, Yeaman S. 2022. Haploid, diploid, and pooled exome capture recapitulate features of biology and paralogy in two non-model tree species. *Molecular Ecology Resources* 22: 225–238.
- Lorenzo O, Piqueras R, Sánchez-Serrano JJ, Solano R. 2003. Ethylene Response Factor1 integrates signals from ethylene and jasmonate pathways in plant defense. *Plant Cell* 15: 165–178.
- Lucek K, Willi Y. 2021. Drivers of linkage disequilibrium across a species' geographic range. *PLoS Genetics* 17: e1009477.
- Ma Q-H, Xu Y. 2008. Characterization of a caffeic acid 3-O-methyltransferase from wheat and its function in lignin biosynthesis. *Biochimie* 90: 515–524.
- Maguire DA, Kanaskie A, Voelker W, Johnson R, Johnson G. 2002. Growth of young Douglas-fir plantations across a gradient in Swiss needle cast severity. *Western Journal of Applied Forestry* 17: 86–95.
- Manter DK, Bond BJ, Kavanagh KL, Rosso PH, Filip GM. 2000. Pseudothecia of Swiss needle cast fungus, *Phaeocryptopus gaeumannii*, physically block stomata of Douglas-fir, reducing CO₂ assimilation. *New Phytologist* 148: 481–491.
- Manter DK, Bond BJ, Kavanagh KL, Stone JK, Filip GM. 2003. Modelling the impacts of the foliar pathogen, *Phaeocryptopus gaeumannii*, on Douglas-fir physiology: net canopy carbon assimilation, needle abscission and growth. *Ecological Modelling* 164: 211–226.
- Marroni F, Pinosio S, Zaina G, Fogolari F, Felice N, Cattonaro F, Morgante M. 2011. Nucleotide diversity and linkage disequilibrium in *Populus nigra* cinnamyl alcohol dehydrogenase (CAD4) gene. *Tree Genetics & Genomes* 7: 1011–1023.
- Maynard Smith J, Haigh J. 1974. The hitch-hiking effect of a favourable gene. *Genetics Research* 23: 23–35.
- McKenna A, Hanna M, Banks E, Sivachenko A, Cibulskis K, Kernysky A, Garimella K, Altshuler D, Gabriel S, Daly M *et al.* 2010. The Genome Analysis Toolkit: a MapReduce framework for analyzing next-generation DNA sequencing data. *Genome Research* 20: 1297–1303.
- Miller RNG, Costa Alves GS, Van Sluys M-A. 2017. Plant immunity: unravelling the complexity of plant responses to biotic stresses. *Annals of Botany* 119: 681–687.
- Mir AA, Park S-Y, Abu Sadat M, Kim S, Choi J, Jeon J, Lee Y-H. 2015. Systematic characterization of the peroxidase gene family provides new insights into fungal pathogenicity in *Magnaporthe oryzae*. *Scientific Reports* 5: 11831.
- Mishina TE, Zeier J. 2006. The Arabidopsis flavin-dependent monooxygenase FMO1 is an essential component of biologically induced systemic acquired resistance. *Plant Physiology* 141: 1666–1675.
- Mitchell-Olds T, Willis JH, Goldstein DB. 2007. Which evolutionary processes influence natural genetic variation for phenotypic traits? *Nature Reviews Genetics* 8: 845–856.
- Montwé D, Elder B, Socha P, Wyatt J, Noshad D, Feau N, Hamelin R, Stoeher M, Ehrling J. 2021. Swiss needle cast tolerance in British Columbia's coastal Douglas-fir breeding population. *Forestry: An International Journal of Forest Research* 94: 193–203.
- Neale DB, McGuire PE, Wheeler NC, Stevens KA, Crepeau MW, Cardeno C, Zimin AV, Puiu D, Pertea GM, Sezen UU *et al.* 2017. The Douglas-fir genome sequence reveals specialization of the photosynthetic apparatus in Pinaceae. *G3: Genes, Genomes, Genetics* 7: 3157–3167.
- Nielsen R. 2005. Molecular signatures of natural selection. *Annual Review of Genetics* 39: 197–218.
- Nurmberg PL, Knox KA, Yun B-W, Morris PC, Shafiei R, Hudson A, Loake GJ. 2007. The developmental selector AS1 is an evolutionarily conserved regulator of the plant immune response. *Proceedings of the National Academy of Sciences, USA* 104: 18795–18800.

- Pagán I, García-Arenal F. 2018. Tolerance to plant pathogens: theory and experimental evidence. *International Journal of Molecular Sciences* 19: 810.
- Pandey S, Nelson DC, Assmann SM. 2009. Two novel GPCR-type G proteins are abscisic acid receptors in Arabidopsis. *Cell* 136: 136–148.
- Panikashvili D, Shi JX, Schreiber L, Aharoni A. 2009. The Arabidopsis DCR encoding a soluble BAHD acyltransferase is required for cutin polyester formation and seed hydration properties. *Plant Physiology* 151: 1773–1789.
- Parker AK. 1970. Effect of relative humidity and temperature on needle cast disease of Douglas fir. *Phytopathology* 60: 1270.
- Parker MT, Knop K, Zacharakis V, Sherwood AV, Tomé D, Yu X, Martin PGP, Beynon J, Michaels SD, Barton GJ *et al.* 2021. Widespread premature transcription termination of *Arabidopsis thaliana* NLR genes by the spen protein FPA. *eLife* 10: e65537.
- Ptak SE, Voelpel K, Przeworski M. 2004. Insights into recombination from patterns of linkage disequilibrium in humans. *Genetics* 167: 387–397.
- Remington DL, Thornsberry JM, Matsuoka Y, Wilson LM, Whitt SR, Doebley J, Kresovich S, Goodman MM, Buckler ES. 2001. Structure of linkage disequilibrium and phenotypic associations in the maize genome. *Proceedings of the National Academy of Sciences, USA* 98: 11479–11484.
- Restif O, Koella JC. 2004. Concurrent evolution of resistance and tolerance to pathogens. *The American Naturalist* 164: E90–E102.
- Ritókóvá G, Shaw DC, Filip G, Kanaskie A, Browning J, Norlander D. 2016. Swiss Needle Cast in Western Oregon Douglas-fir plantations: 20-year monitoring results. *Forests* 7: 155.
- Sakai H, Hua J, Chen QG, Chang C, Medrano LJ, Bleecker AB, Meyerowitz EM. 1998. ETR2 is an ETR1-like gene involved in ethylene signaling in Arabidopsis. *Proceedings of the National Academy of Sciences, USA* 95: 5812–5817.
- Serrano M, Coluccia F, Torres M, L'Haridon F, Métraux J-P. 2014. The cuticle and plant defense to pathogens. *Frontiers in Plant Science* 5: 274.
- Sharma E, Anand G, Kapoor R. 2017. Terpenoids in plant and arbuscular mycorrhiza-reinforced defence against herbivorous insects. *Annals of Botany* 119: 791–801.
- Shaw DC, Filip GM, Kanaskie A, Maguire DA, Littke WA. 2011. Managing an epidemic of Swiss needle cast in the Douglas-fir region of Oregon: the role of the Swiss needle cast cooperative. *Journal of Forestry* 109: 109–119.
- Shaw DC, Ritókóvá G, Lan Y-H, Mainwaring DB, Russo A, Comeleo R, Navarro S, Norlander D, Smith B. 2021. Persistence of the Swiss needle cast outbreak in Oregon coastal Douglas-fir and new insights from research and monitoring. *Journal of Forestry* 119: 407–421.
- Smith KF, Sax DF, Lafferty KD. 2006. Evidence for the role of infectious disease in species extinction and endangerment. *Conservation Biology* 20: 1349–1357.
- Stone J. 2018. Swiss needle cast. In: Hansen EM, Lewis KJ, Chastagner GA, eds. *Compendium of conifer diseases*. St Paul, MN, USA: APS Press, 111–114.
- Stone JK, Coop LB, Manter DK. 2008. Predicting effects of climate change on Swiss needle cast disease severity in Pacific Northwest forests. *Canadian Journal of Plant Pathology* 30: 169–176.
- Temel F, Johnson GR, Adams WT. 2005. Early genetic testing of coastal Douglas-fir for Swiss needle cast tolerance. *Canadian Journal of Forest Research* 35: 521–529.
- Temel F, Johnson GR, Stone JK. 2004. The relationship between Swiss needle cast symptom severity and level of *Phaeocryptopus gaeumannii* colonization in coastal Douglas-fir (*Pseudotsuga menziesii* var. *menziesii*). *Forest Pathology* 34: 383–394.
- Tuladhar P, Sasidharan S, Saudagar P. 2021. 17 – Role of phenols and polyphenols in plant defense response to biotic and abiotic stresses. In: Jogaiah S, ed. *Biocontrol agents and secondary metabolites*. Sawston, UK: Woodhead, 419–441.
- Wang J, Chai J. 2020. Structural insights into the plant immune receptors PRRs and NLRs1. *Plant Physiology* 182: 1566–1581.
- Wang R-S, Pandey S, Li S, Gookin TE, Zhao Z, Albert R, Assmann SM. 2011. Common and unique elements of the ABA-regulated transcriptome of Arabidopsis guard cells. *BMC Genomics* 12: 216.
- Wegrzyn JL, Liechty JD, Stevens KA, Wu L-S, Loopstra CA, Vasquez-Gross HA, Dougherty WM, Lin BY, Zieve JJ, Martínez-García PJ *et al.* 2014. Unique features of the loblolly pine (*Pinus taeda* L.) megagenome revealed through sequence annotation. *Genetics* 196: 891–909.
- Wilhelmi N, Bennett PI, Shaw DC, Stone JK. 2021. *Rhabdocone needle cast of Douglas-fir*. Forest insect and disease leaflet 190. Portland, OR, USA: USDA Forest Service.
- Wilhelmi NP, Shaw DC, Harrington CA, Clair JBS, Ganio LM. 2017. Climate of seed source affects susceptibility of coastal Douglas-fir to foliage diseases. *Ecosphere* 8: e02011.
- Yang S, Li J, Zhang X, Zhang Q, Huang J, Chen J-Q, Hartl DL, Tian D. 2013. Rapidly evolving R genes in diverse grass species confer resistance to rice blast disease. *Proceedings of the National Academy of Sciences, USA* 110: 18572–18577.
- Yeaman S, Hodgins KA, Lotterhos KE, Suren H, Nadeau S, Degner JC, Nurkowski KA, Smets P, Wang T, Gray LK *et al.* 2016. Convergent local adaptation to climate in distantly related conifers. *Science* 353: 23–26.
- Young ND. 1996. QTL mapping and quantitative disease resistance in plants. *Annual Review of Phytopathology* 34: 479–501.
- Zhang H, Gao Z, Zheng X, Zhang Z. 2012. The role of G-proteins in plant immunity. *Plant Signaling & Behavior* 7: 1284–1288.
- Zhang X, Fend Z, Zhao L, Liu S, Wei F, Shi Y, Feng H, Zhu H. 2020. Succinate dehydrogenase SDH1–1 positively regulates cotton resistance to *Verticillium dahliae* through a salicylic acid pathway. *Journal of Cotton Research* 3: 12.
- Zhu C, Gore M, Buckler ES, Yu J. 2008. Status and prospects of association mapping in plants. *The Plant Genome* 1: 1–20.
- Zhu Z, Xu F, Zhang Y, Cheng YT, Wiermer M, Li X, Zhang Y. 2010. Arabidopsis resistance protein SNC1 activates immune responses through association with a transcriptional corepressor. *Proceedings of the National Academy of Sciences, USA* 107: 13960–13965.

Supporting Information

Additional Supporting Information may be found online in the Supporting Information section at the end of the article.

Fig. S1 Map of sampling/planting sites for this study for both SNC and RNC, see Table S1 for more details.

Fig. S2 Health index of individuals assigned SNC tolerant or intolerant based on measure phenotypes.

Fig. S3 PCA of SNP allele frequencies.

Fig. S4 Distribution of SNPs per gene.

Fig. S5 Distribution of number of SNPs per gene vs number of GWAS outlier SNPs per gene.

Fig. S6 Decay of linkage disequilibrium calculated.

Notes S1 Forest health survey protocol followed by foresters during sampling and assignment of tolerant, intolerant, and resistant phenotypes of Douglas-fir trees.

Table S1 Sampling location information.

Table S2 DNA extraction details and sample pooling information.

Table S3 Significant SNC and RNC SNPs and gene annotations and gene ontology annotations and enrichment and per gene summary of SNPs.

Table S4 Number of samples assigned to *Nothophaeocryptopus gaeumannii* genetic lineage 1 and 2 in six Douglas-fir sites.

Please note: Wiley is not responsible for the content or functionality of any Supporting Information supplied by the authors. Any queries (other than missing material) should be directed to the *New Phytologist* Central Office.